P-244

Preclinical and Clinical Characterization of PA-001, a Macrocyclic Peptide That Targets the S2 Subunit of SARS-CoV-2 Spike Protein

Hidetomo Kitamura[1,2], Haruaki Kurasaki[1,2], Masaki Ohuchi[1], Kazutaka Nagatomo[1], Hirofumi Ohashi[3], Naoko Iwata-Yoshikawa[4], Nozomi Shiwa-Sudo[4], Yusuke Sakai[4], Naoki Kawamura[1], Shoko Ito[1,2], Takuma Yonemura[5], Takeshi Chiyoda[5], Asuka Yamamoto[5], Akihito Shimoi[6], Keiichi Masuya[1,2], Noriyo Nagata[4], Koichi Watashi[3], Tadaki Suzuki[4], Masato Murakami[1]

[1]PeptiDream Inc., [2]PeptiAID Inc., Kawasaki, Japan; [3]Research Center for Drug and Vaccine Development,
[4]Department of Pathology, National Institute of Infectious Diseases, Tokyo, Japan;
[5]SOUSEIKAI Sumida Hospital, Tokyo, Japan; [6]Ina Research Inc., Ina, Japan

(1) Introduction

- ✓ Coronavirus disease 2019 (COVID-19) is caused by severe acute respiratory syndrome coronavirus 2 (SARS-CoV-2). So far, >770 million confirmed COVID-19 cases, including >6.9 million deaths, have been reported worldwide [1].
- ✓ Although several COVID-19 drugs, including antivirals, monoclonal antibodies, and immunomodulators, have been approved or granted emergency use authorization (EUA), there are limitations in the existing drugs (e.g., drug-drug interactions, potential risks of toxicity, and emergence of drug-resistant mutants) [2].
- ✓ Since various mutations of SARS-CoV-2 continue to emerge [3], there is an unmet clinical need for broad-spectrum treatments.
- ✓ SARS-CoV-2 spike (S) protein consists of the receptor-binding subunit S1 and the membrane-fusion subunit S2. While emergence of mutations frequently occurs in the S1 subunit, the S2 subunit is highly conserved [4].
- ✓ Employing PeptiDream's proprietary technology Peptide Discovery Platform System (PDPS) [5], we identified PA-001, a macrocyclic peptide that targets the S2 subunit of SARS-CoV-2 S protein. Here we report the preclinical studies and clinical characterization (safety and pharmacokinetics) of PA-001 as a potential therapeutic agent for COVID-19.

(3) *In Vitro* Antiviral Activity of PA-001 *(Workshop 4-4)*

Table 2. Broad-spectrum antiviral activity of PA-001 against SARS-CoV-2 strains (IC_{90} values, nM)

Compound	SARS-CoV-2 strain					
	WK-521 (WT)	QK002 (Alpha)	TY8-612 (Beta)	TY7-501 (Gamma)	TY11-927 (Delta)	TY38-873 (Omicron)
PA-001	2.7	7.6	2.5	2.9	9.6	1.7
Remdesivir	4400	2800	4500	2600	5400	5700

In vitro antiviral activity was evaluated in VeroE6/TMPRSS2 cells infected with SARS-CoV-2 by quantification of viral E gene in the culture supernatant using RT-qPCR

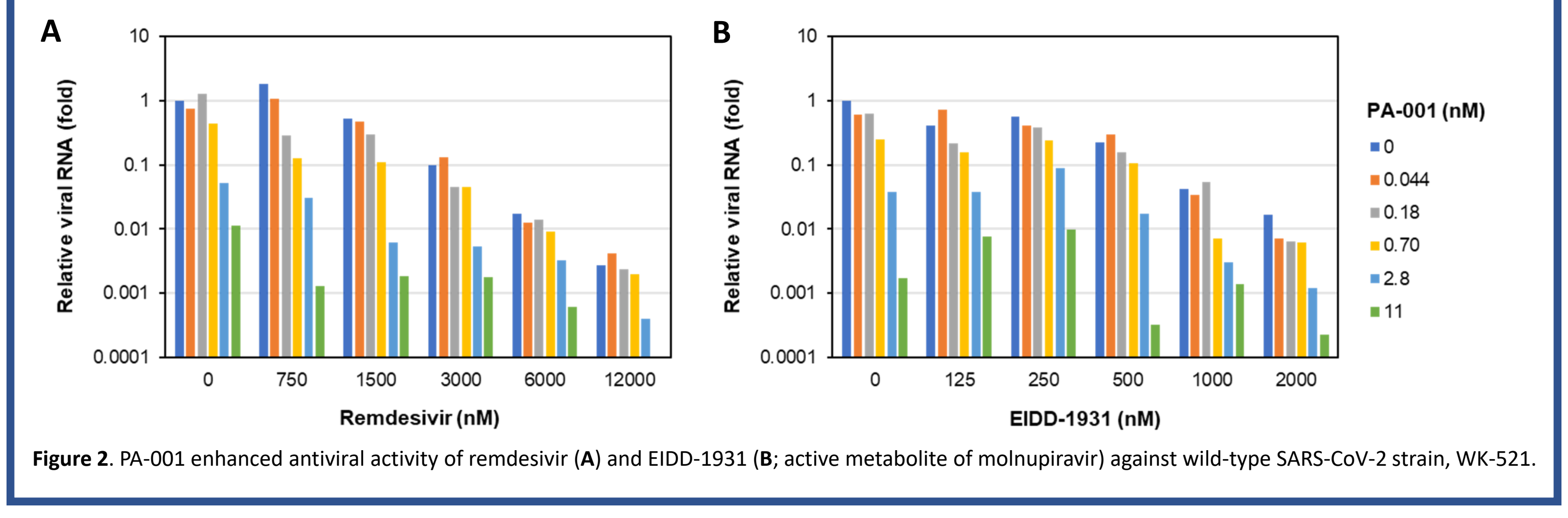

Figure 2. PA-001 enhanced antiviral activity of remdesivir (**A**) and EIDD-1931 (**B**; active metabolite of molnupiravir) against wild-type SARS-CoV-2 strain, WK-521.

(4) *In Vivo* Efficacy of PA-001 in Hamster Model

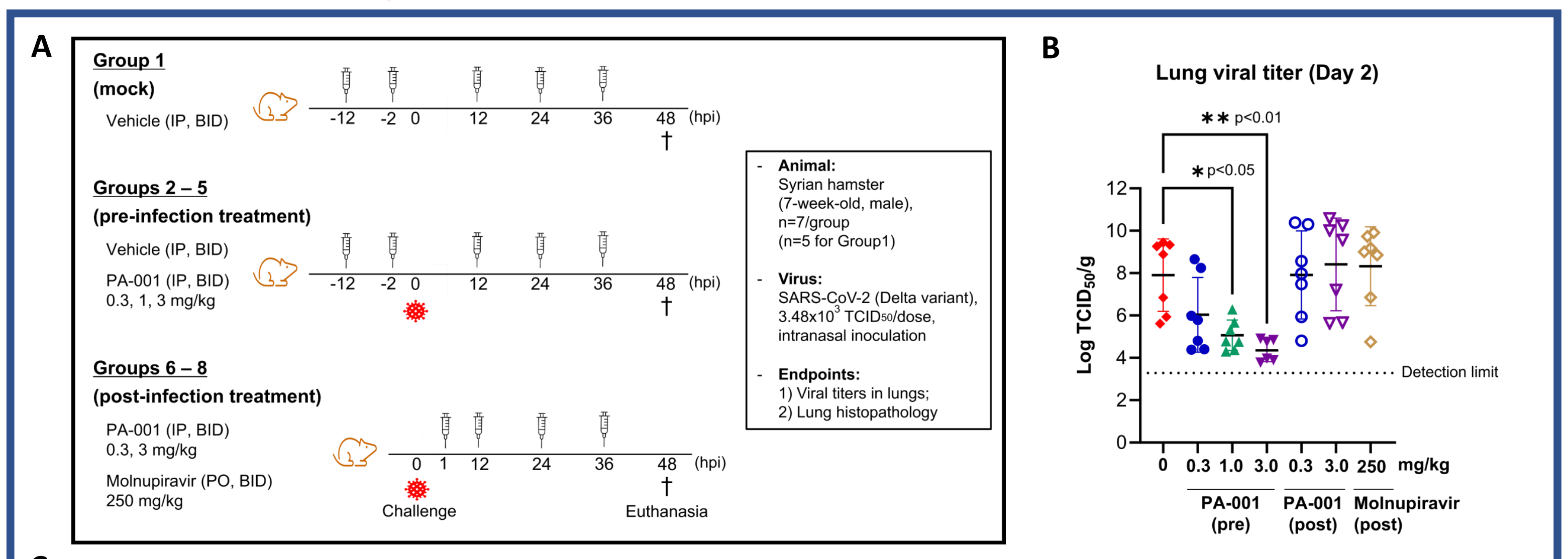

C

Inflammation (mixed or mononuclear cell alveolar, bronchoalveolar and/or interstitial)

	Mock	Vehicle (pre)	PA-001 (0.3 mg/kg, pre)	PA-001 (1 mg/kg, pre)	PA-001 (3 mg/kg, pre)	PA-001 (0.3 mg/kg, post)	PA-001 (3 mg/kg, post)	Molnupiravir (250 mg/kg, post)
Unremarkable	●●●●●	-	-	●	●●	-	-	-
Minimal	-	-	●	●●●	●●	-	●●●●●●	-
Mild	-	●●●●●●●	●●●●●●	●●●	●●	●●●●●●	●	●●●●●●●
Moderate	-	-	-	-	-	●	-	-

Inflammation (vascular/perivascular)

	Mock	Vehicle (pre)	PA-001 (0.3 mg/kg, pre)	PA-001 (1 mg/kg, pre)	PA-001 (3 mg/kg, pre)	PA-001 (0.3 mg/kg, post)	PA-001 (3 mg/kg, post)	Molnupiravir (250 mg/kg, post)
Unremarkable	●●●●●	●	-	●	●●●	-	●●●	●
Minimal	-	●	●●●●●●	●●●●	●●●	-	●●●	●●●●●
Mild	-	●●●●	●	●●	-	●●●●●●●	●	●
Moderate	-	●	-	-	-	-	-	-

Necrosis

	Mock	Vehicle (pre)	PA-001 (0.3 mg/kg, pre)	PA-001 (1 mg/kg, pre)	PA-001 (3 mg/kg, pre)	PA-001 (0.3 mg/kg, post)	PA-001 (3 mg/kg, post)	Molnupiravir (250 mg/kg, post)
Unremarkable	●●●●●	-	●●●●●●	●●●●●●	●●●●●●	-	●●●●●●●	-
Minimal	-	●	●	●	-	●●●●●●	-	●●●●●●●
Mild	-	●●●●●●	-	-	-	●	-	-
Moderate	-	-	-	-	-	-	-	-

Figure 3.
(**A**) Schematic design of the efficacy study in a SARS-CoV-2-infected hamster model.
(**B**) Prophylactic treatment with PA-001 reduced viral titers in lungs.
Mean with SD, one-way ANOVA with Dunnett's multiple comparison test.
(**C**) Histopathology revealed that PA-001 reduced SARS-CoV-2-related microscopic findings in lungs at 2 days post-infection, superior to molnupiravir.

(5) *In Vitro* Therapeutic Efficacy of PA-001 in Lethal Mouse Model *(Workshop 4-4)*

A

Objectives:
1. Evaluation of the therapeutic efficacy of PA-001 alone at the anticipated clinical dose
2. Evaluation of the combination effect of PA-001 with the remdesivir metabolite, GS-441524
3. Comparison of the efficacy of PA-001 with that of molnupiravir at the anticipated clinical doses

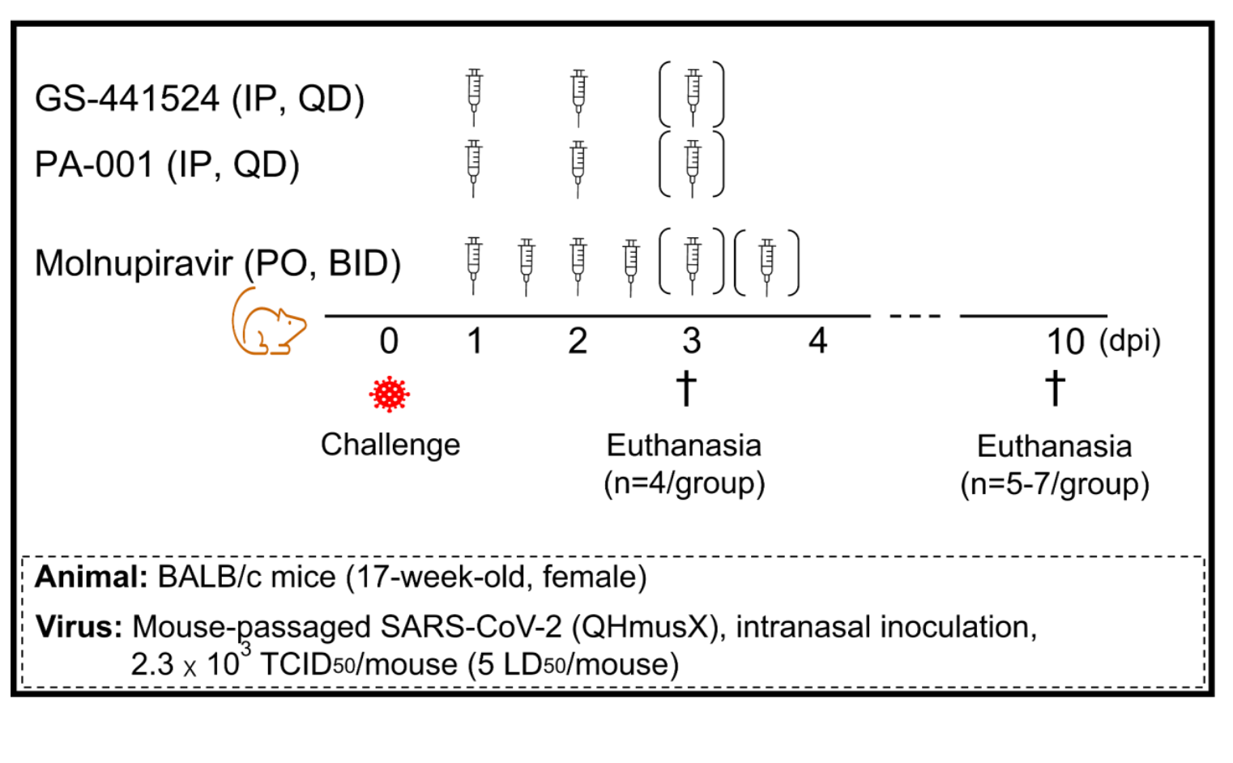

Animal: BALB/c mice (17-week-old, female)
Virus: Mouse-passaged SARS-CoV-2 (QHmusX), intranasal inoculation, 2.3 x 10^3 TCID50/mouse (5 LD50/mouse)

Treatment groups:
1. Vehicle
2. GS-441524, High (25, 12.5, 12.5 mg/kg)
3. GS-441524, High (25, 12.5, 12.5 mg/kg) + PA-001 (26 mg/kg)
4. GS-441524, Low (6.25, 3.13, 3.13 mg/kg) + PA-001 (26 mg/kg)
5. PA-001 (26 mg/kg)
6. Molnupiravir (164 mg/kg)

Endpoints:
1. Survival rate (0 – 10 dpi, daily)
2. Body weight (0 – 10 dpi, daily)
3. Viral titers in lungs ($TCID_{50}$, 3 dpi)
4. Cytokine levels in lungs (3 dpi)
5. Lung weight (3 dpi)

Therapeutic intervention started at 1 dpi

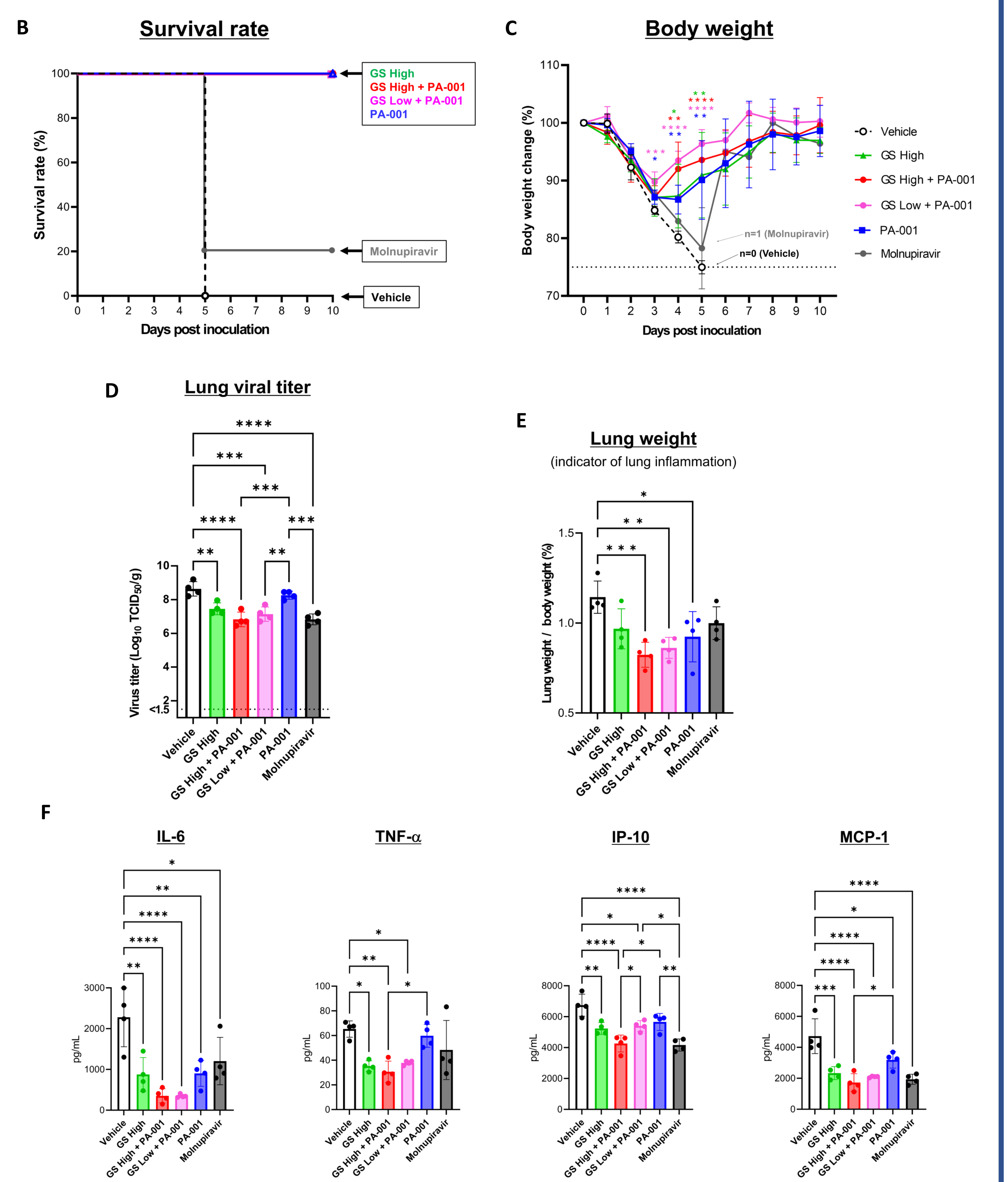

Figure 4. (**A**) Schematic design of the efficacy study in a lethal mouse model infected with a mouse-passaged SARS-CoV-2 strain, QHmusX [6]. PA-001 and/or GS-441524, or molnupiravir were therapeutically administered for 3 consecutive days started at 1 day post-infection (dpi). The nucleoside metabolite of remdesivir, GS-441524, was alternatively used due to the poor plasma stability of remdesivir in mouse [7]. (**B**) Therapeutic administration of PA-001 completely rescued mice from SARS-CoV-2-caused death at the anticipated clinical dose, while 80% of molnupiravir-administered mice and all vehicle-administered mice died. (**C**) Treatment with PA-001 alone significantly suppressed body weight loss superior to molnupiravir, and this effect was enhanced in combination with GS-441524.
(**D**) Reduction in the lung viral titer by PA-001 was enhanced when combined with GS-441524. (**E, F**) PA-001 alone reduced lung weight, an indicator of lung inflammation (**E**), and pro-inflammatory cytokine levels, including IL-6 and MCP-1, in lungs at 3 dpi (**F**), and these effects were enhanced in combination with GS-441524. Taken together, this study showed (1) the *in vivo* therapeutic efficacy of PA-001 as single agent, (2) effectiveness of combination therapy with GS-441524, and (3) superiority to molnupiravir in clinical symptom recovery.
(**B**) ****p<0.0001, vs. Vehicle, Log-rank test. (**C**) Mean with SD, *p<0.05, **p<0.01, ***p<0.001, ****p<0.0001, vs. Vehicle, Dunnett's multiple comparison test.
(**D-F**) Mean with SD, *p<0.05, **p<0.01, ***p<0.001, ****p<0.0001, one-way ANOVA with Šídák's (**D**), Dunnett's (**E**; vs. Vehicle), or Tukey's (**F**) multiple comparison tests.

(2) Identification of PA-001 as a Selective Spike S2 Binder *(Workshop 4-4)*

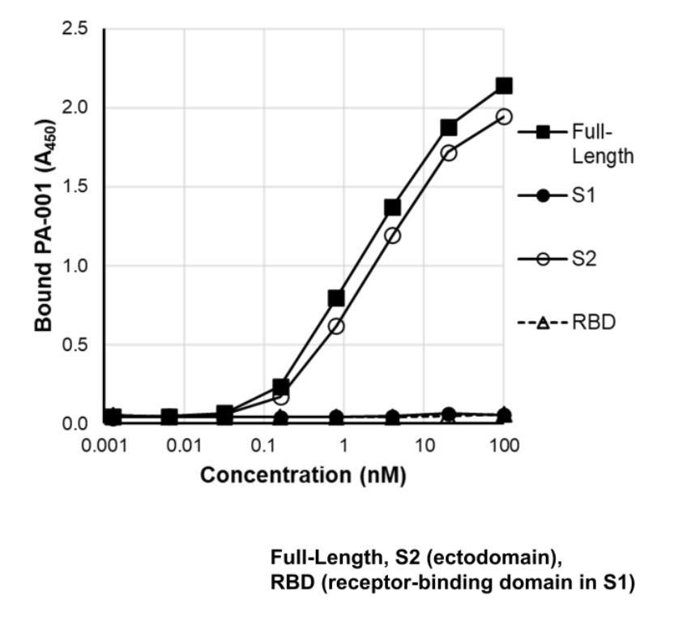

Full-Length, S2 (ectodomain), RBD (receptor-binding domain in S1)

Figure 1.
PA-001 bound to the S2 subunit of SARS-CoV-2 S protein, but not the S1 subunit, in ELISA. A high binding affinity of PA-001 for SARS-CoV-2 S protein was confirmed by SPR analysis (K_D: 1.8 nM).

Table 1. Enzyme and radioligand binding assays with the SafetyScreen panel composed of mammalian molecules (showing high selectivity of PA-001 for SARS-CoV-2 S protein)

Family	Assay Name	Species	% Inhibition	Conc.	Family	Assay Name	Species	% Inhibition	Conc.	IC_{50}
GPCR	Adenosine A2A	human	-4	10 µM	Ion Channel	Calcium Channel L-Type, Dihydropyridine	rat	-3	10 µM	
GPCR	Adrenergic α1A	human	-7	10 µM	Ion Channel	GABAA, Flunitrazepam, Central	rat	10	10 µM	
GPCR	Adrenergic α2A	human	0	10 µM	Ion Channel	Glutamate, NMDA, Agonism	rat	19	10 µM	>300 µM
GPCR	Adrenergic β1	human	-6	10 µM	Ion Channel	Potassium Channel [KA]	rat	-3	10 µM	
GPCR	Adrenergic β2	human	-2	10 µM	Ion Channel	Potassium Channel hERG, [3H]Dofetilide	human	-4	10 µM	
GPCR	Cannabinoid CB1	human	8	10 µM	Ion Channel	Sodium Channel, Site 2	rat	1	10 µM	
GPCR	Cannabinoid CB2	human	-3	10 µM	Ion Channel	Calcium Channel L-Type, Benzothiazepine	rat	1	10 µM	
GPCR	Cholecystokinin CCK1 (CCKA)	human	9	10 µM	Ion Channel	Calcium Channel L-Type, Phenylalkylamine	rat	-7	10 µM	
GPCR	Dopamine D1	human	6	10 µM	Ion Channel	Calcium Channel N-Type	rat	-4	10 µM	
GPCR	Dopamine D2S	human	7	10 µM	Ion Channel	GABAA, Chloride Channel, TBOB	rat	1	10 µM	
GPCR	Endothelin ETA	human	-1	10 µM	Ion Channel	GABAA, Ro-15-1788, Hippocampus	rat	22	10 µM	>300 µM
GPCR	Histamine H1	human	13	10 µM	Ion Channel	GABAB1A	human	17	10 µM	>300 µM
GPCR	Histamine H2	human	-11	10 µM	Ion Channel	Glutamate, AMPA	rat	-8	10 µM	
GPCR	Muscarinic M1	human	9	10 µM	Ion Channel	Glutamate, Kainate	rat	-4	10 µM	
GPCR	Muscarinic M2	human	-5	10 µM	Ion Channel	Glutamate, Metabotropic, mGlu5	human	12	10 µM	
GPCR	Muscarinic M3	human	-6	10 µM	Ion Channel	Glutamate, NMDA, Glycine	rat	1	10 µM	
GPCR	Opiate δ1 (OP1, DOP)	human	13	10 µM	Ion Channel	Glutamate, NMDA, Phencyclidine	rat	-4	10 µM	
GPCR	Opiate κ (OP2, KOP)	human	14	10 µM	Ion Channel	Glutamate, NMDA, Polyamine	rat	-4	10 µM	
GPCR	Opiate μ (OP3, MOP)	human	-3	10 µM	Ion Channel	Glycine, Strychnine-Sensitive	rat	0	10 µM	
GPCR	Serotonin (5-Hydroxytryptamine) 5-HT1A	human	0	10 µM	Ion Channel	Potassium Channel [KATP]	hamster	-3	10 µM	
GPCR	Serotonin (5-Hydroxytryptamine) 5-HT1B	human	-1	10 µM	Kinase	Protein Tyrosine Kinase, LCK	human	-3	10 µM	
GPCR	Serotonin (5-Hydroxytryptamine) 5-HT2A	human	-4	10 µM	Kinase	Protein Serine/Threonine Kinase, PRKCA (PKCα)	human	19	10 µM	
GPCR	Serotonin (5-Hydroxytryptamine) 5-HT2B	human	-10	10 µM	Kinase	Protein Tyrosine Kinase, Insulin Receptor	human	25	10 µM	
GPCR	Serotonin (5-Hydroxytryptamine) 5-HT3	human	-10	10 µM	Lipid Metabolism	Cyclooxygenase COX-1	human	-4	10 µM	
GPCR	Vasopressin V1A	human	0	10 µM	Lipid Metabolism	Cyclooxygenase COX-2	human	3	10 µM	
GPCR	Adenosine A1	human	-6	10 µM	Neurotransmitter Metabolism	Cholinesterase, Acetyl, ACES	human	-26	10 µM	
GPCR	Adrenergic α1B	human	11	10 µM	Neurotransmitter Metabolism	Monoamine Oxidase MAO-A	human	-2	10 µM	
GPCR	Adrenergic α1D	human	-6	10 µM	Neurotransmitter Metabolism	Nicotinic Acetylcholine α4β2, Cytisine	human	4	10 µM	
GPCR	Adrenergic α2B	human	0	10 µM	Neurotransmitter Metabolism	Monoamine Oxidase MAO-B	human	40	10 µM	246 µM
GPCR	Angiotensin AT1	human	4	10 µM	NHR	Androgen (Testosterone)	human	0	10 µM	
GPCR	Bradykinin B2	human	11	10 µM	NHR	Glucocorticoid	human	27	10 µM	68.4 µM
GPCR	Chemokine CCR1	human	-7	10 µM	NHR	Estrogen ERα	human	-3	10 µM	
GPCR	Chemokine CXCR2 (IL-8RB)	human	9	10 µM	NHR	PPARγ	human	0	10 µM	
GPCR	Cholecystokinin CCK2 (CCKB)	human	4	10 µM	NHR	Progesterone PR-B	human	8	10 µM	
GPCR	Dopamine D2L	human	0	10 µM	PDE	Phosphodiesterase PDE3A	human	-5	10 µM	
GPCR	Leukotriene, Cysteinyl CysLT1	human	-1	10 µM	PDE	Phosphodiesterase PDE4D2	human	2	10 µM	
GPCR	Melanocortin MC1	human	-2	10 µM	Protease	Peptidase, Angiotensin Converting Enzyme	human	19	10 µM	207 µM
GPCR	Melanocortin MC4	human	-14	10 µM	Protease	Peptidase, CTSG (Cathepsin G)	human	56	10 µM	6.87 µM
GPCR	Muscarinic M4	human	10	10 µM	Transporter	Transporter, Dopamine (DAT)	human	-5	10 µM	
GPCR	Neuropeptide Y Y1	human	-4	10 µM	Transporter	Transporter, Norepinephrine (NET)	human	-7	10 µM	
GPCR	Nicotinic Acetylcholine α1, Bungarotoxin	human	2	10 µM	Transporter	Transporter, Serotonin (5-Hydroxytryptamine) (SERT)	human	8	10 µM	
GPCR	Nicotinic Acetylcholine α3β4	human	-6	10 µM						
GPCR	Platelet Activating Factor (PAF)	human	0	10 µM	Transporter	ATPase, Na+/K+, Heart, Pig	pig	8	10 µM	
GPCR	Serotonin (5-Hydroxytryptamine) 5-HT2C	human	9	10 µM	Transporter	Transporter, Adenosine	guinea pig	15	10 µM	>300 µM
GPCR	Tachykinin NK1	human	3	10 µM	Transporter	Transporter, GABA	rat	-8	10 µM	

(6) Safety and Pharmacokinetics of PA-001 in Healthy Japanese Subjects (jRCTs031210601)

Study Overview

- ✓ The specified clinical trial was conducted in Japan to evaluate the safety and pharmacokinetics, following a single intravenous administration of PA-001.
- ✓ Six healthy Japanese adult male volunteers were enrolled for each cohort (Step 1 to 5).
- ✓ PA-001 was administered at 0.3, 1, 2, 4 or 8 mg in 50 mL via intravenous infusion for 1 hour.

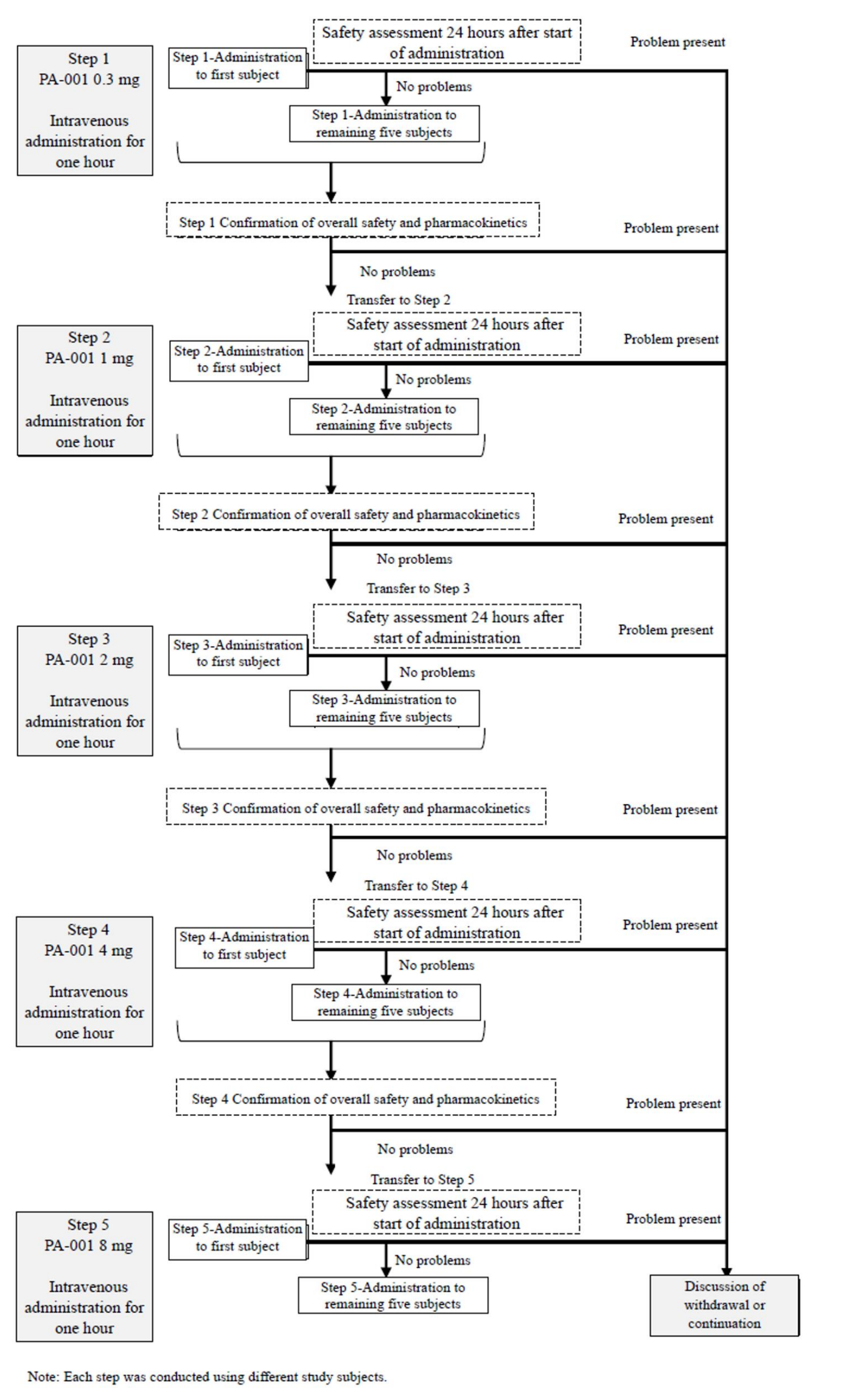

Note: Each step was conducted using different study subjects.

Figure 5. Overview of step transfer

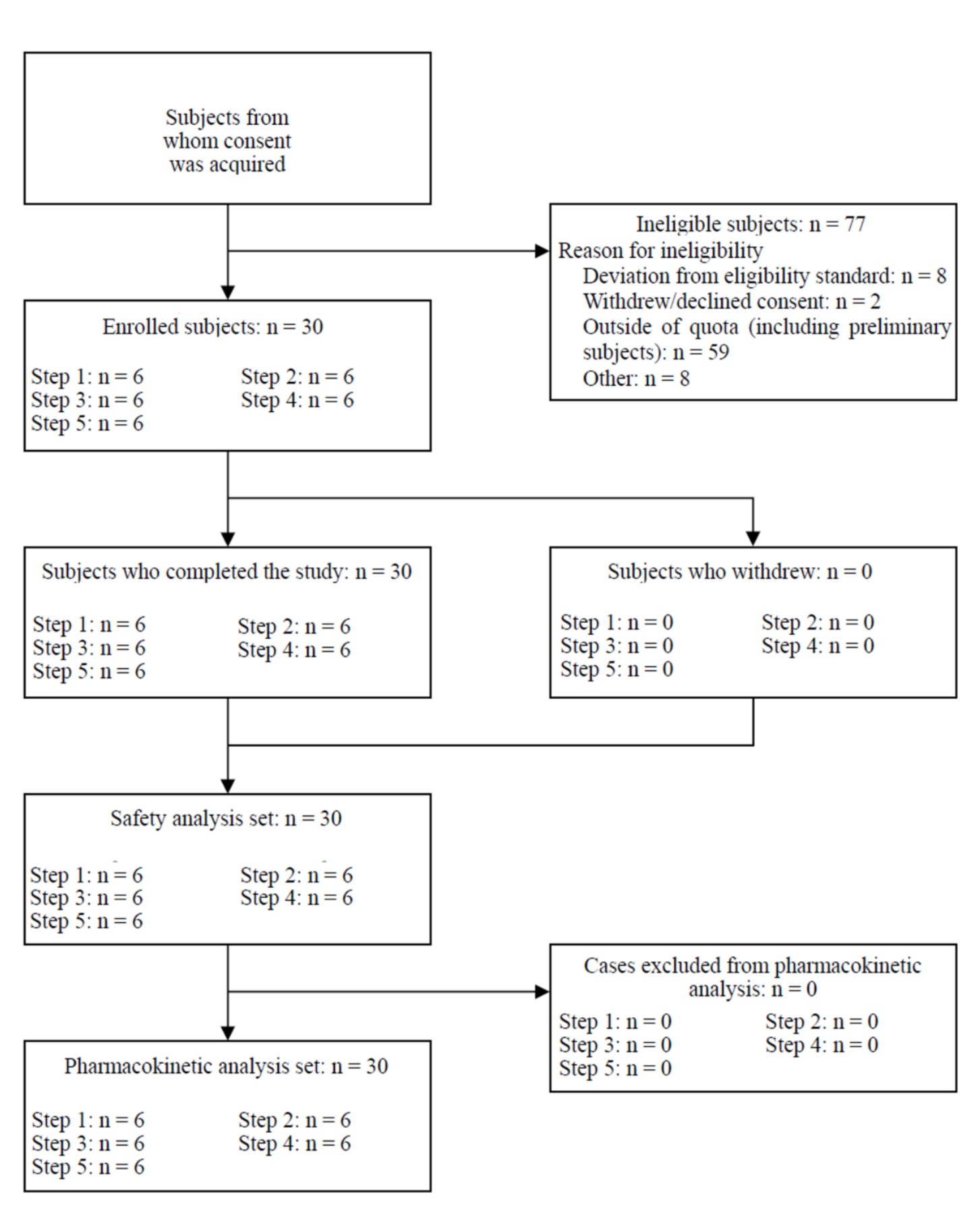

Figure 6. Classification and breakdown of study subjects

Safety (Primary Endpoints)

- ✓ No serious adverse events were observed in this clinical research.
- ✓ Adverse events occurred in 1 subject from Step 3 (n=6) and in 2 subjects from Step 5 (n=6), while no adverse events were observed in other cohorts.
- ✓ Observed adverse events include extremity pain (1 subject from Step 3), increase in C-reactive protein levels (1 subject from Step 5) and increase in neutrophil count (1 subject from Step 5).
- ✓ All adverse events were mild, and subjects recovered without any additional treatment.
- ✓ All adverse events were not causally related to PA-001.

Table 3-1. Overview of adverse events

	Step 1	Step 2	Step 3	Step 4	Step 5
	(n = 6)	(n = 6)	(n = 6)	(n = 6)	(n = 6)
Adverse events	0 (0.0) 0	0 (0.0) 0	1 (16.7) 1	0 (0.0) 0	1 (16.7) 2
Adverse drug reactions	0 (0.0) 0	0 (0.0) 0	0 (0.0) 0	0 (0.0) 0	0 (0.0) 0
Serious adverse events	0 (0.0) 0	0 (0.0) 0	0 (0.0) 0	0 (0.0) 0	0 (0.0) 0
Serious adverse drug reactions	0 (0.0) 0	0 (0.0) 0	0 (0.0) 0	0 (0.0) 0	0 (0.0) 0
Adverse events leading to withdrawal from study	0 (0.0) 0	0 (0.0) 0	0 (0.0) 0	0 (0.0) 0	0 (0.0) 0

Number of subjects (incidence %) Number of cases

Table 3-2. Frequency of occurrence of adverse events

System Organ Class	Step 1	Step 2	Step 3	Step 4	Step 5
Preferred Term	(n = 6)	(n = 6)	(n = 6)	(n = 6)	(n = 6)
Adverse events	0 (0.0) 0	0 (0.0) 0	1 (16.7) 1	0 (0.0) 0	1 (16.7) 2
Investigations	0 (0.0) 0	0 (0.0) 0	0 (0.0) 0	0 (0.0) 0	1 (16.7) 2
C-reactive protein increased	0 (0.0) 0	0 (0.0) 0	0 (0.0) 0	0 (0.0) 0	1 (16.7) 1
Neutrophil percentage increased	0 (0.0) 0	0 (0.0) 0	0 (0.0) 0	0 (0.0) 0	1 (16.7) 1
Musculoskeletal and connective tissue disorders	0 (0.0) 0	0 (0.0) 0	1 (16.7) 1	0 (0.0) 0	0 (0.0) 0
Pain in extremity	0 (0.0) 0	0 (0.0) 0	1 (16.7) 1	0 (0.0) 0	0 (0.0) 0

Number of subjects (incidence %) Number of cases

Table 3-3. Frequency of occurrence of adverse drug reactions

System Organ Class	Step 1	Step 2	Step 3	Step 4	Step 5
Preferred Term	(n = 6)	(n = 6)	(n = 6)	(n = 6)	(n = 6)
Adverse drug reactions	0 (0.0) 0	0 (0.0) 0	0 (0.0) 0	0 (0.0) 0	0 (0.0) 0

Number of subjects (incidence %) Number of cases

Pharmacokinetics (Secondary Endpoints)

- ✓ In all cohorts, the plasma concentrations of PA-001 reached C_{max} at 1 hour after administration and decreased with $T_{1/2}$ of 2.30 to 3.39 hours. Elimination rate constant (K_{el}), CL, V_{ss} and mean residence time (MRT) of PA-001 were 0.216 to 0.309/h, 2,340 to 2,850 mL/h, 9,090 to 11,700 mL and 3.19 to 4.27 h, respectively, and there was no significant difference among each cohort.
- ✓ The C_{max} and AUC_{inf} of PA-001 were confirmed to increase in a dose-proportional manner. Dose proportionality was found at the doses ranged from 0.3 to 8 mg by power model..

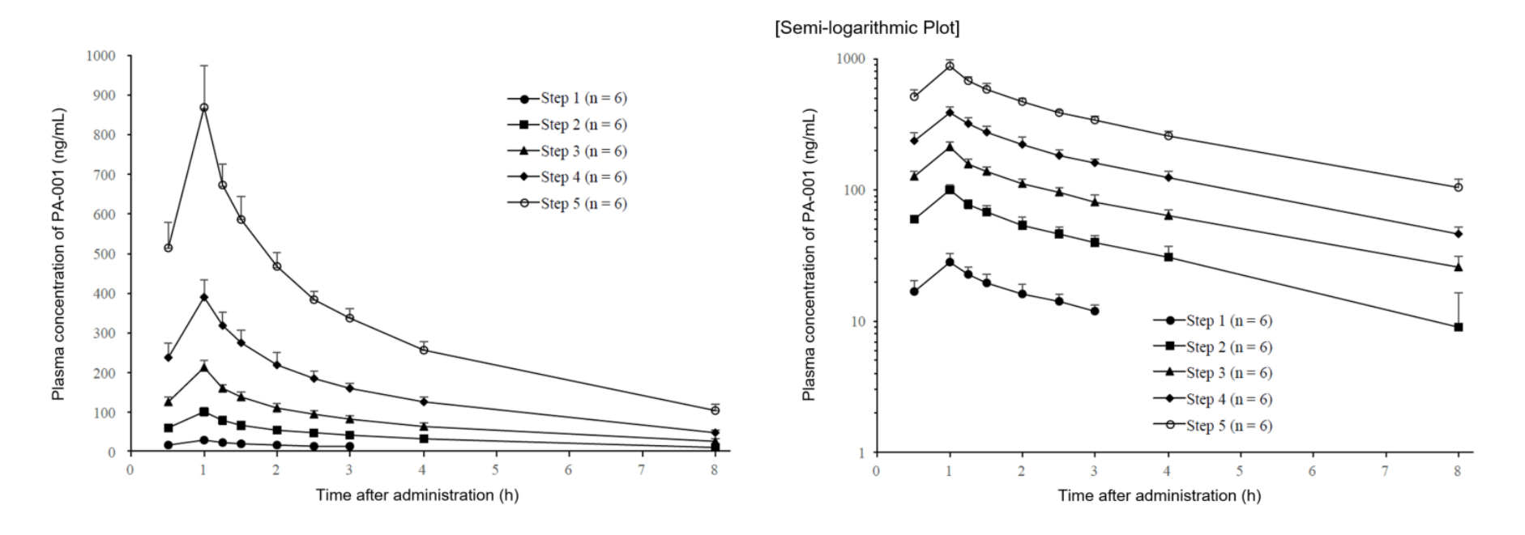

Figure 6. Time-plasma concentration profiles of PA-001 after single IV administration
Mean with SD. Other than the two subjects from Step 5, all were under the lower limit of quantification after 24 hours. Plasma concentrations of PA-001 at 24 h post-dose and later were below the lower limit of quantification in all subjects except 2 subjects dosed 8 mg of PA-001.

Table 4. Pharmacokinetic parameters of PA-001 in plasma

Pharmacokinetic Parameters	Step 1	Step 2	Step 3	Step 4	Step 5
	0.3 mg	1 mg	2 mg	4 mg	8 mg
	(n = 6)	(n = 6)	(n = 6)	(n = 6)	(n = 6)
C_{max} (ng/mL)	28.1 (4.8)	98.9 (10.3)	213 (18)	389 (44)	868 (107)
T_{max} (h)	1.00 (0.00)	1.00 (0.00)	1.00 (0.00)	1.00 (0.00)	1.00 (0.00)
k_{el} (1/h)	0.309 (0.051)	0.309 (0.051)	0.309 (0.051)	0.309 (0.051)	0.309 (0.051)
$T_{1/2}$ (h)	2.30 (0.44)	2.68 (0.63)	3.06 (0.28)	2.80 (0.14)	3.39 (0.90)
AUC_{inf} (ng·h/mL)	90.7 (16.5)	328 (71)	712 (84)	1330 (150)	3000 (390)
CL_{tot} (mL/h)	2780 (380)	2470 (630)	2340 (250)	2850 (310)	2510 (590)
V_{ss} (mL)	9090 (1170)	9090 (1040)	10300 (1100)	11500 (1000)	11700 (700)
MRT (h)	3.19 (0.58)	3.19 (0.58)	3.19 (0.58)	3.19 (0.58)	3.19 (0.58)

AUC_{inf} = area under the concentration-time curve from time 0 to infinity; CL_{tot} = total clearance; C_{max} = maximum concentration; k_{el} = elimination rate constant; MRT = mean residence time; $t_{1/2}$ = half-life; T_{max} = time to maximum concentration; V_{ss} = volume of distribution at steady state. Note: Data are represented as mean (standard deviation).

(7) Summary and Outlook

- ✓ PA-001 selectively bound to the S2 subunit of SARS-CoV-2 S protein (K_D: 1.8 nM).
- ✓ PA-001 exhibited broad *in vitro* antiviral activity against wild-type and mutant SARS-CoV-2 strains, including alpha, beta, gamma, delta and omicron variants (IC_{90}: 1.7 – 9.6 nM).
- ✓ PA-001 reduced viral titers in lungs and attenuated the lung pathology in a SARS-CoV-2-infected hamster model.
- ✓ PA-001 showed therapeutic efficacy alone and in combination with GS-441524, the nucleoside metabolite of remdesivir, at the anticipated clinical doses in a SARS-CoV-2-infected lethal mouse model with severe acute pneumonia, superior to molnupiravir.
- ✓ The safety and linear plasma exposure of PA-001 were confirmed up to 8 mg, when administered as a single intravenous dose over 1 hour to healthy adult males (jRCTs031210601).
- ✓ Our data suggest that the S2-targeting peptide PA-001 has a potential to become a novel drug with a unique mechanism of action for the treatment of COVID-19.
- ✓ Good Laboratory Practice (GLP) toxicology and safety pharmacology studies of PA-001 for Phase 1 clinical trial have been completed.
- ✓ Investigational New Drug (IND) submission for PA-001 is currently in preparation to initiate Phase 1 clinical trial.

(8) References

[1] WHO, as of Sep. 6th, 2023; https://covid19.who.int/; [2] Li G. et al., Nat. Rev. Drug Discov. 22, 449-475, 2023; Toussi S.S. et al., Nat. Rev. Microbiol. 8, 771–786, 2023;
[3] Markov P.V. et al., Nat. Rev. Microbiol. 21, 361-379, 2023; [4] Carabelli A.M. et al., Nat. Rev. Microbiol. 21, 162-177, 2023;
[5] Corporate Presentation, PeptiDream Inc., Aug. 1st, 2023; https://www.peptidream.com/en/ir/news/;
[6] Iwata-Yoshikawa N. et al., Sci. Adv. 8, eabh3827, 2022; [7] Sheahan T.P. et al., Sci. Transl. Med. 9, eaal3653, 2017

(9) Acknowledgments

- ✓ This research was supported in part by AMED Research Program on Emerging and Re-emerging Infectious Diseases (JP22fk0108529 to Koichi Watashi, PhD and JP23fk0108645 to Hirofumi Ohashi, PhD at NIID).
- ✓ Takayuki Nagasawa, Junpei Yamamoto, Katsuma Matsui, Masatoshi Matsumoto, Hikaru Shimizu, Koji Yoshida, and Tatsuro Kawamura (PeptiDream Inc.) contributed to the identification and characterization of PA-001.
- ✓ Tatsuro Kawamura and Tomoaki Higuchi (PeptiDream Inc.) contributed to the preparation and editing of this poster, respectively.
- ✓ Setsuo Hasegawa, MD, PhD (Pharmaspur Inc.) greatly contributed to conducting the clinical research.

(10) Conflict of Interest (COI)

H.Kitamura, H.Kurasaki, M.O., K.N., N.K., S.I., and M.M. are employees of PeptiDream Inc. H.Kitamura, H.Kurasaki, and S.I. are employees on temporary assignment at PeptiAID Inc. A.S. was an employee of Ina Research Inc. during the study. K.M. is the president at PeptiAID Inc. and the director and chief operating officer (COO) at PeptiDream Inc.